Research Square

Preprints are preliminary reports that have not undergone peer review.
They should not be considered conclusive, used to inform clinical practice,
or referenced by the media as validated information.

Evaluation the maximum ceiling temperature and temperature longitudinal decay in a ventilated bifurcation tunnel with uphill mainline

Zhiwen Wang
Suzhou University of Technology
Youbo Huang
ybhuang@cqust.edu.cn
Chongqing University of Science and Technology
Yujia Zhao
Suzhou University of Technology
Jingtai Shi
Suzhou University of Technology
Mengmeng Xie
Chongqing University of Science and Technology

Research Article

Keywords: Tunnel fire, Maximum temperature, Bifurcation tunnel, longitudinal ventilation

Posted Date: June 4th, 2026

DOI: https://doi.org/10.21203/rs.3.rs-9735798/v1

License: This work is licensed under a Creative Commons Attribution 4.0 International License.
Read Full License

Additional Declarations: No competing interests reported.

Evaluation the maximum ceiling temperature and temperature longitudinal decay in a ventilated bifurcation tunnel with uphill mainline

Zhiwen Wang[a], Youbo Huang[b*], Yujia Zhao[a], Jingtai Shi[a**], Mengmeng Xie[b]

[a] School of Materials Engineering, Suzhou University of Technology, Suzhou, Jiangsu 215500, P. R. China

[b] College of Safety Engineering, Chongqing University of Science and Technology, Chongqing 401331, China

*Corresponding author: ybhuang@cqust.edu.cn (Y.B. Huang), shijingtai@163.com (J. T. Shi).

Abstract

Fire in complex tunnels poses unique threats to urban public safety and infrastructure. This study systematically investigates the fire characteristics in a branched tunnel with sloped mainline, focused on the effect of mainline slope, longitudinal ventilation and heat release rate on temperature distribution in mainline and ramp. Results reveal lower maximum ceiling temperature under higher airflow velocity. Greater heat release rate significantly elevates the maximum ceiling temperature in mainline. The maximum ceiling temperature rise is changed as the variation of mainline slope. The induced airflow velocity was employed to correlate the dimensionless temperature rise that the 0.36 power of $\sin\theta$ was utilized to normalize the induced airflow velocity. The temperature beneath the mainline ceiling decreases with higher airflow velocity and is slightly influenced by the mainline slope. The Fr was utilized to correlate the dimensionless temperature longitudinal decay along mainline ceiling that sum of two exponential equations were established. The effect of mainline slope on temperature longitudinal decay along ramp ceiling is limited, but the heat release rate plays an important role. The prediction model for temperature distribution in ramp is developed based on the exponential equation. This study contributes to developing robust fire safety strategies and risk assessment in complex branched tunnel conditions.

Keywords: Tunnel fire, Maximum temperature, Bifurcation tunnel, longitudinal ventilation

1. Introduction

The tunnel, as an irreplaceable component of urban infrastructure, have been extensively constructed to alleviate the urban traffic congestion, and provide urban operation efficiency [1-2]. Tunnel fire pose a significant threat on tunnel operation safety due to causing serious casualties and facilities damage [3-4]. For instance, Yanhou tunnel fire in Shanxi province in 2024 caused 40 deaths and 12 injures [5], Maoliling tunnel fire in Zhejiang province in 2019 caused 5 deaths and 31 injures. Tunnel as a long-narrow confined space restricted the heat and toxic smoke diffusion that results in the high-temperature toxic smoke becoming a crucial factor for the death and injure, even over 85% deaths in tunnel fire due to the smoke [6]. Recently, the complex tunnel composed with multiple branched structures has been extensively developed to connect the urban ground transportation and underground road. The multiple passways for smoke movement and airflow in those tunnels give rise to the difficulty of smoke control and evacuation, which bring about more serious of hazards consequences. Therefore, it's urgent to unveil the smoke movement and temperature

profile in complex urban tunnel fire.

The smoke propagation and temperature distribution in tunnels have been attached great importance in previous study. Alpert [7-8] described the plume of smoke movement in a confined space and established the theoretical model for maximum temperature of ceiling jet under natural condition. Kurioka et al. [9] derived the model formula for maximum temperature beneath the tunnel ceiling by taking the effect of longitudinal ventilation into account that utilizing the non-dimensional heat release rate and Froude number to correlate the maximum ceiling temperature. Hu et al [10] conducted the full-scale experiments and numerical modelling to validate this empirical model with difference less than 4.5%. But there is no application of this formula for maximum temperature under natural conditions. Ingason et al. [11] proposed the two piecewise functions for maximum smoke temperature beneath the tunnel ceiling that neglected the influence of ventilation during dimensionless ventilation velocity less than 0.19. Hu et al. [12] upgraded this model to predict the maximum ceiling temperature under influence of blockage. The existing empirical model mainly utilized the heat release rate and ventilation velocity, which represent the energy intensity and cooling effect, to correlate the maximum ceiling temperature. The multiple factors would impact the cooling effect and heat distribution beneath the tunnel ceiling, further changing the ceiling temperature. Thus, the tunnel slope [13], fire source position [14], sub-atmospheric [15], double fire source [16] and branched structure [17] has been considered to optimize the prediction model for maximum ceiling temperature. But the coupling effect of mainline slope and bifurcation structure on temperature distribution is complexed that has not been unveiled. The previous study only revealed the effect of ramp slope on smoke propagation and temperature distribution in a naturally branched tunnel [18]. There is still a research gap on multiple tunnel slopes and ventilation on temperature distribution in branched tunnels.

The smoke temperature decays with distance between maximum temperature position two sides. Ingason and Li [19] developed an exponential function for dimensional temperature distribution along the tunnel ceiling with constant coefficient of 0.9575, furtherly, the sum of two exponential equations was developed and can well predict longitudinal temperature. The temperature longitudinal decay relates to the CO concentration along tunnel ceiling [20] and be normalized utilizing dimensionless distance x/H [21] with constant coefficient of 1 that lager than 0.9575. Zhang et al. [22] given impetus to the longitudinal temperature prediction model by modified the dimensionless distance utilizing flame length. The asymmetric attenuation of longitudinal temperature would occur between fire source two sides under the action of ventilation and tunnel slope. Hu et al. [23] compared the full-scale experimental results with calculated temperature by Delichatsios proposed model [24], which taken the longitudinal ventilation velocity into account. The induced airflow occurs in sloped tunnels that smoke is toward uphill direction and attaches great importance to temperature attenuation. Ji et al [25] investigated the upstream temperature rise and developed an empirical model under natural condition. Yu et al. [6] numerically studied the combination effect of tunnel slope and ventilation on smoke distribution in ordinary tunnel fire but without the quantification for longitudinal temperature. The inertial force

and stack effect induced by buoyancy would significantly change the temperature longitudinal decay upstream and downstream. In current, the complex urban tunnel has been extensively constructed that composed with bifurcation structure. The temperature longitudinal decay in those branched tunnel cannot be correlated by utilizing the previous model for ordinary single tunnel because of the combination effect of divergent flow and multiple slope region [26]. Thus, Cheng et al. [18] proposed an empirical model to predict the longitudinal temperature beneath the mainline tunnel ceiling by taking the ramp slope into account. Li et al. [27] claimed that the fire source transverse location at joint node played an important role in temperature distribution and quantified it utilizing the exponential function. Huang et al. [28] studied the temperature longitudinal decay in mainline and ramp under ventilated condition in horizontal tunnel. However, the inclined mainline always occurred to connect with ground transportation. The combination effect of stack effect, divergent flow and longitudinal ventilation on smoke movement is complex and has been barely studied. There is still a lack of prediction models for the temperature distribution in this branched tunnel that causes difficulties in tunnel design, emergency management and risk assessment. Thus, to fill this gap, it is necessary to investigate the temperature longitudinal distribution in branched tunnel with mainline slope and ventilation conditions.

In view of this, the present study carried out a series of small-scale experiments to investigate the smoke movement and ceiling temperature distribution in the branched tunnel. The combination effect of ventilation velocity and mainline slope on ceiling temperature has been revealed and proposed the mathematical model for temperature longitudinal decay. The findings of this study contribute to tunnel fire dynamics and provide theoretical guidance for design of ventilation systems in tunnels.

2. Experimental approach

In present study, a 1:20 scale-down branched tunnel was utilized to conduct fire experiments, which were controlled by the Froude criterion. The branched tunnel consisted of mainline region and ramp with cross dimension of 0.5 m (width) × 0.25 m (height), where the tunnel length of mainline and ramp were 10 m and 4 m, as shown in Fig.1. To visually observe the fire process, the front tunnel wall was covered by the 10 mm thickness fireproof glass with thermal conductivity of 1.1 W/(m·k). The other tunnel walls were constructed by 5 mm thickness of steel plate with thermal conductivity of 17 W/(m·k). The bifurcation angle between mainline and ramp maintains 30°. The mainline slope before shunting ranges from 0% to 7% with interval of 2%.

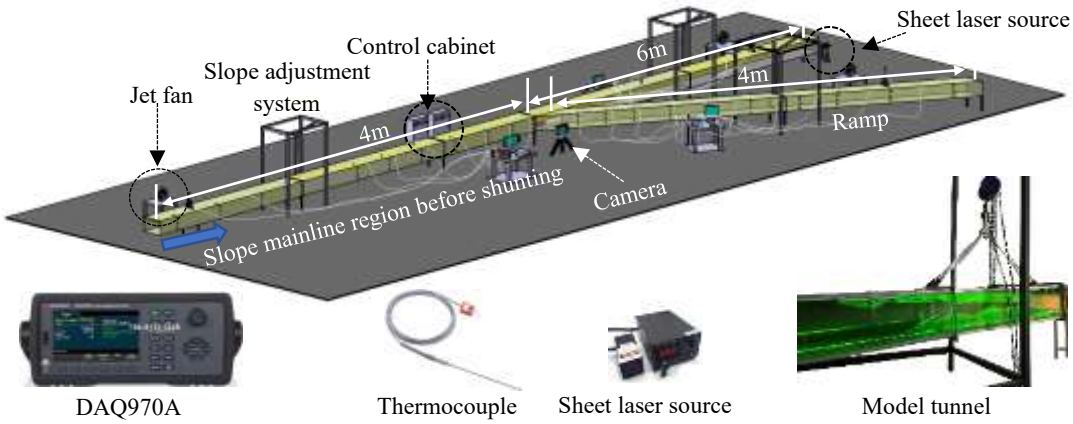


Fig.1 Schematic diagram of small-scale experimental setup.

The thermocouple with diameter of 1 mm was utilized to detect the ceiling temperature that the measurement ranges from 0 ℃ to 1500 ℃ with accuracy of 1 ℃. Five thermocouple trees were placed between fire source two sides with interval of 0.2 m, where each thermocouple tree consisted of three probes. Beyond of this region, the thermocouples were longitudinal mounted along mainline and ramp beneath the ceiling 0.1 m with longitudinal spacing of 0.4 m, the detail information can be found in previous study [3]. A data acquisition system of Keysight DAQ970A was employed to collect the temperature signal and transferred to a personal computer. A frequency fan was utilized to supply the longitudinal ventilation from downhill mainline entrance that the velocity was measured by a hot-wire anemometer (Kanomax KA12). The measurement range of hot-wire anemometers is from 0 m/s to 20 m/s with accuracy of 0.01 m/s. The airflow velocity away from downhill entrance 2.05 m and 2.95 m were detected where the cross-section velocity full development. An electronic balance was employed to weigh the fuel mass with accuracy of 0.01 g, furtherly, the mass loss rate was calculated to deduce the heat release rate at quasi-steady state, expressed as Eq. (1). The n-heptane with the combustion heat of 44.6 MJ/kg [29] was employed as the fuel. Three heat release rates including 1.12 kW, 1.64 kW and 2.8 kW were considered in present study. Five airflow velocity in downhill mainline region was conducted for each heat release rate and mainline slope. The experimental conditions were summarized in Table 1 for various HRRs, mainline slope and airflow velocity.

$$Q = \chi \dot{m} \Delta H \tag{1}$$

where Q is the heat release rate (kW), χ is the combustion efficiency 0.92 for n-heptane, $\dot{m}$ is the mass loss rate (kg/s), $\triangle H$ is the combustion heat (kJ/kg).

Table 1 List of the experimental conditions

No.	Bifurcation angle (°)	HRR (kW)	Mainline slope (%)	Ventilation velocity (m/s)
Test A	30	1.12	0, 1, 3, 5, 7	0.10, 0.15, 0.20, 0.3, 0.40

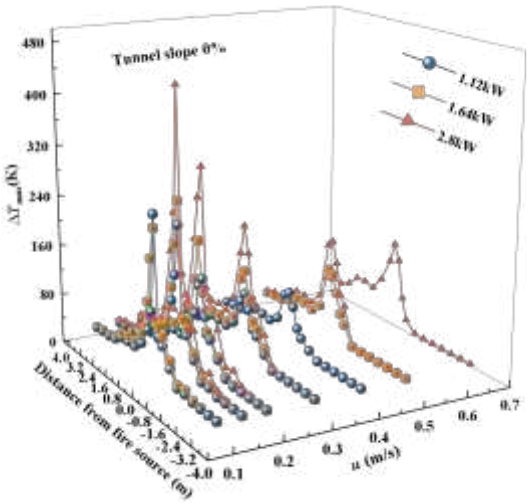
Test B	30	1.64	0, 1, 3, 5, 7	0.10, 0.15, 0.20, 0.30, 0.50
Test C	30	2.80	0, 1, 3, 5, 7	0.15, 0.20, 0.30, 0.50, 0.65

3. Results and discussion

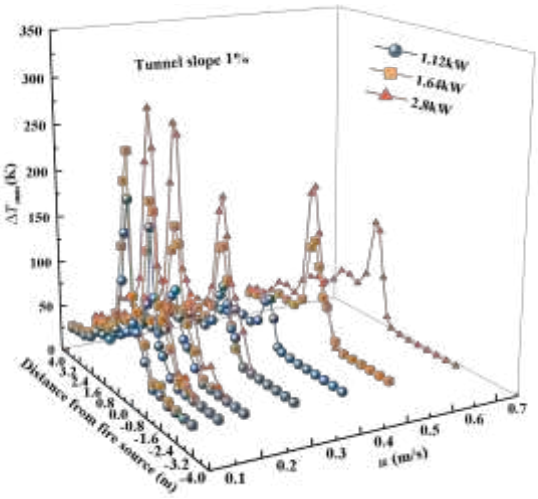
3.1 Temperature longitudinal distribution in mainline

Fig.2 exhibits the longitudinal temperature beneath the tunnel ceiling under ventilation conditions. The temperature decays gradually between fire source two sides that upstream temperature decays faster than downstream value, this phenomenon becomes more obvious with higher ventilation velocity. In horizontal tunnels with natural ventilation, the driving force of smoke movement is the thermal pressure as the temperature difference between smoke and ambient air. While the airflow is mainly governed by the local negative-pressure effect near the fire source [30]. Because of the asymmetrical air entrainment from fire source two sides including only mainline portal before shunting and mainline tunnel portal combined with ramps after shunting, the smoke layer slightly inclines to the portal sides with larger opening area [31]. In longitudinal ventilation tunnel, the inertial force of ventilation causes the hot smoke to preferentially exhaust from the downstream portal as the local negative-pressure effect induced by the asymmetrical air entrainment. Owing to the ventilation velocity suppresses the local negative-pressure effect near fire source, a pressure imbalance is more prominent even leading to the maximum ceiling temperature position shifted to downstream. That demonstrated the non-orthogonal ventilation effect of longitudinal airflow and buoyancy. The stronger the airflow velocity, the lower the ceiling temperature occurred. That indicates the cooling effect of ventilation suppressing the combustion assisting effect.

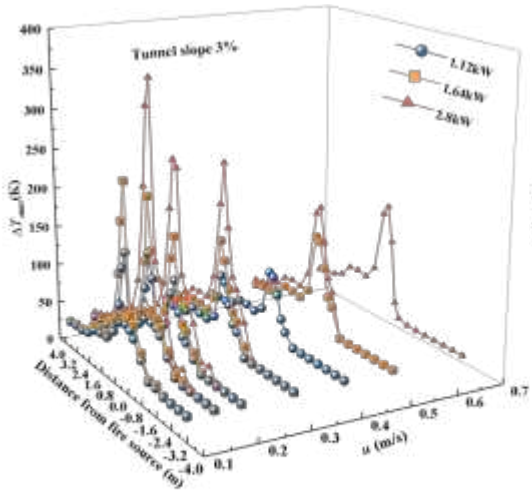
From Fig. 2, the mainline slope before shunting exerts an unfavorable influence on temperature longitudinal decay beneath the tunnel ceiling. The smoke temperature at upstream decays faster with steeper uphill mainline but this influence is limited. The elevation difference between lower portal to location of fire source at joint node cause the rising hot smoke to preferentially discharge from the high portals [30]. The induced airflow is formed in sloped tunnel as the stack effect [32], which combined with the longitudinal ventilation suppresses the oxygen supply effect and deflects plume toward to high-slope portal. Under the circumstance, the longitudinal temperature weakens and the ceiling impingement point shifts further toward the high-slope side. Therefore, the smoke temperature distribution in bifurcation tunnel is affected by the asymmetrical air entrainment from multiple portals, ventilation velocity and mainline slopes.



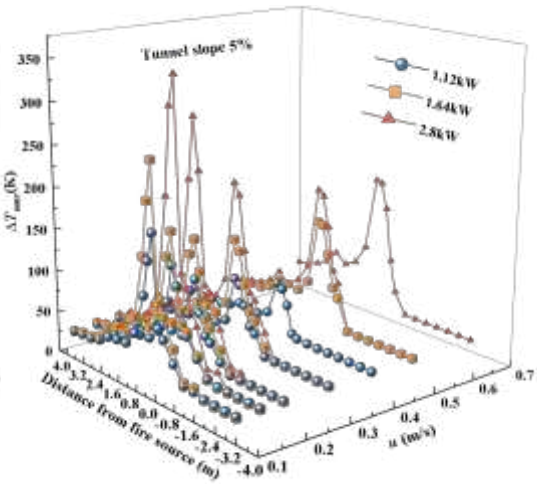
(a) Horizontal mainline tunnel



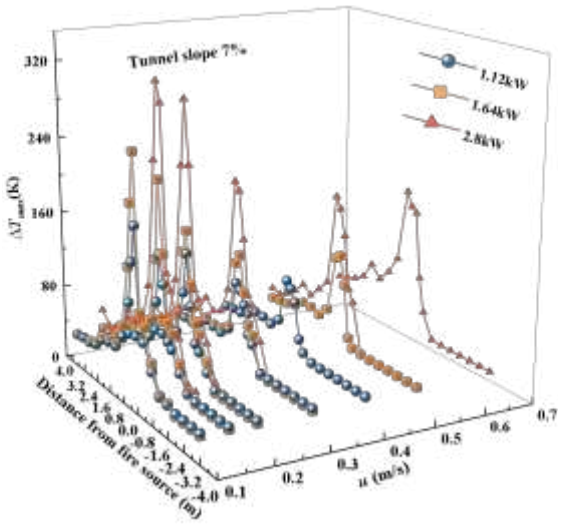
(b) Mainline slope of 1%



(c) Mainline slope of 3%



(d) Mainline slope of 5%



(e) Mainline slope of 7%

Fig.2 Temperature longitudinal decay under different mainline slopes.

The maximum ceiling temperature rise in horizontally bifurcation tunnel has been normalized in previous study [3], expressed as Eq. (2).

$$\Delta T_{\max} = \begin{cases} 6.81 Q_{H_{ef}}^{*2/3} T_0, & u' \le 0.19 \\ 1.71 u'^{-5/6} Q_{H_{ef}}^{*2/3} T_0, & u' > 0.19 \end{cases} \quad (2)$$

where $\triangle T_{max}$ is the maximum temperature rise (K), Q^*_{Hef} is the dimensionless heat release rate, $Q^*_{Hef} = Q/(\rho_0 c_p T_0 g^{1/2} H_{ef}^{5/2})$, ρ_0 is the ambient density (kg/m^3), c_p is the air specific heat capacity (kJ/(kg·K)), g is the gravitational acceleration (m/s^2), H_{ef} is the effective height between fire source surface to tunnel ceiling (m), T_0 is the ambient temperature (K), u' is the dimensionless velocity $u' = u/(Qg/b_f \rho_0 c_p T_0)$, b_f is the radios of fire source (m).

But for the inclined mainline, the induced airflow velocity was taken to modify the ventilation velocity u. Meric [33] established a induced airflow velocity regarding global stack effect caused by fires in inclined tunnel under natural condition. The mainline slope has been replaced by the sine of title angle. The induced airflow velocity is expressed as,

$$u_{in} = 22 L^{-0.25} \sin^{0.36}\theta d^{-0.11} Q_c^{0.33} \left(1 - \exp\left(-b_f h\right)\right) \quad (3)$$

where u_{in} is the indued airflow velocity (m/s), L is the tunnel length of inclined region (m), θ is the mainline slope (°), d is the roughness of the tunnel wall (m), Q_c is the convention heat release rate (MW), h is the convection coefficient (W/(m^2·K)).

The $u+u_{in}$ is utilized to replace the ventilation velocity inside tunnel and substitute this velocity into Eq. (2) to predict the maximum temperature rise in branched tunnel with inclined mainline. The prediction of maximum ceiling temperature was calculated utilizing Eq. (2) and compared with the experimental results, as shown in Fig.3. The prediction demonstrates good agreement with experimental data, with most prediction errors remaining within 20%. In addition, the predictions also compared with the calculated value using formula proposed by Huang et al. [3] and experimental results conducted by Chen et al. [18]. The predictions agree well with the previous experimental results, showing a relative error of less than 20%. The previous model also took the induced airflow velocity into account but not considering the effect of heat release rate on induced airflow velocity, thus, there is still a little deviation.

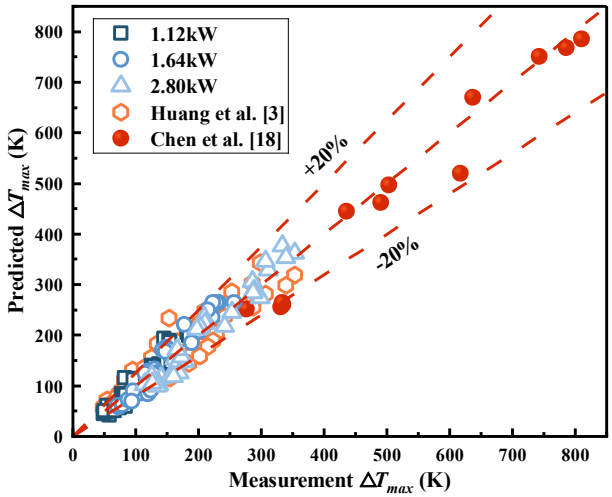


Fig.3 Comparison of $\triangle T_{max}$ (calculated value vs. measurement value).

The temperature longitudinal decay in mainline is influenced by the fire power, tunnel slope and airflow velocity. The dimensionless excess ceiling temperature of $\triangle T_x/\triangle T_{max}$ was introduced to correlate the excess temperature along tunnel ceiling that has been verified following an exponential decay [20]. Hu et al. [34] established a single exponential expression for dimensionless excess ceiling temperature taking the tunnel slope into account, given as Eq. (4). To well normalized the ceiling temperature, the constant coefficient [25] is always loaded in left-hand side of Eq. (5). Furtherly, the sum of two exponential equations was proposed to normalize the ceiling temperature inside branched tunnel [28, 35], expressed as Eq. (5).

$$\frac{\Delta T_x}{\Delta T_{\max}} = e^{-k(x-x_0)} \tag{4}$$

$$\frac{\Delta T_x}{\Delta T_{\max}} = a_1 \exp(b_1 \frac{x-x_{\max}}{H_{ef}}) + a_2 \exp(b_2 \frac{x-x_{\max}}{H_{ef}}) \tag{5}$$

where $\triangle T_x$ is temperature rise at position x (K), k is the coefficient, x_0 is the reference position, a_1 and a_2 are constant, b_1 and b_2 are coefficients.

For the natural condition, the dimensionless ceiling temperature has been directly correlated utilizing the heat release rate [36] but not $\triangle T_{max}$, given as Eq. (6). But this model is invalid for tunnel fire under longitudinal ventilation conditions. Li et al. [37] also directly normalized the ceiling temperature utilizing Q and Richardson number (Ri) based on the single exponential equation, given as Eq. (7).

$$\frac{\Delta T_x}{T_0 Q_{H_{ef}}^{*2/3}} = a_1 \exp(b_1 \frac{x-x_0}{H_{ef}}) + a_2 \exp(b_2 \frac{x-x_0}{H_{ef}}) \tag{6}$$

$$\frac{\Delta T_x}{T_0} \Big/ (Q_{H_{ef}}^{*2/3} Ri^{1/3}) = a + b\,\mathrm{e}^{-k\frac{x-x_0}{H_{ef}}} \tag{7}$$

where Ri is the Richardson number, a and b are coefficients.

From the experimental results, the temperature rise at upstream is limited due to air inflow. Thus, the temperature decay in mainline downstream region is mainly focused. Fig.4 exhibits the relationship between downstream dimensionless excess temperature and $(x\text{-}x_0)/H_{ef}$ for heat release rate of 1.12 kW and mainline slope of 0%. It is obvious that excess temperature decay cannot be normalized using dimensionless values at different ventilation velocities.

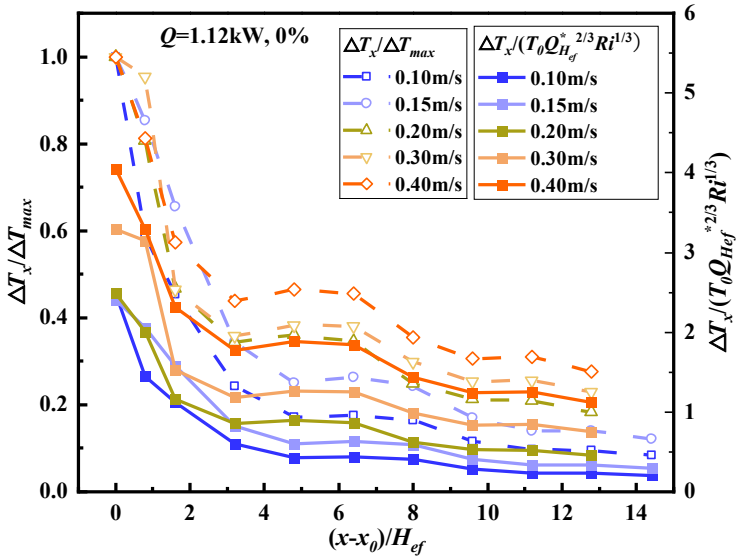
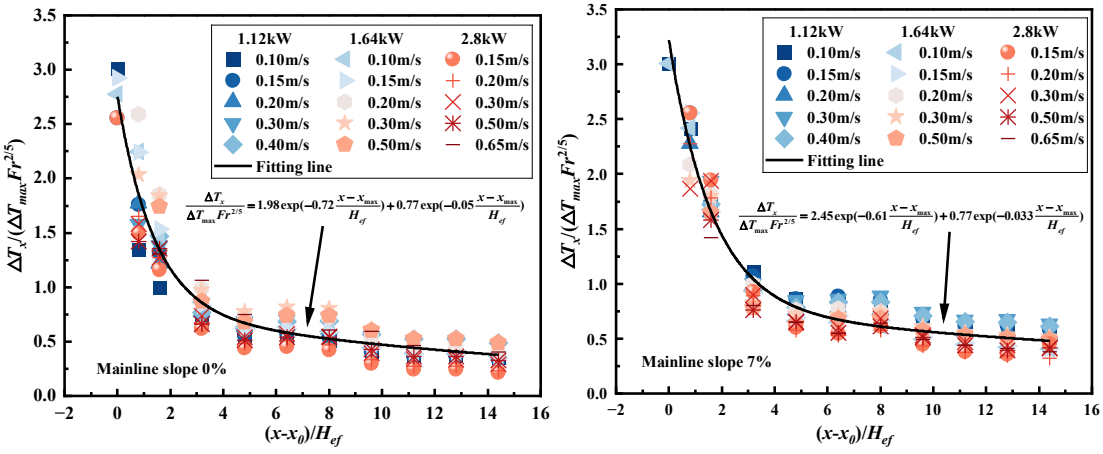


Fig.4 Relationship between dimensinless temeprature rise and distance.

From the Fig.4, the ventilation velocity has a siginificant influence on the temeprature longitudinal decay along the mainline ceiling. Zhao et al. [38] claimed that the temperature longitudinal decay related to the -1/2 power of the *Fr*, where $Fr=u/(gH)^{1/2}$. The research conducted by Kurioka et al. [9] indictade that the -2/5 power of the *Fr* can well correlate the dimenisnoless maximum temeprature rise beneath the tunnel ceiling. Based on the physical mechanism of dimensionless excess ceiling temperature to -2/5 power of the *Fr*, the denominator in equation (5) was promoted taking $Fr^{2/5}$ into account. Thus, the dimensionless excess temeprature can be expressed as $\triangle T_x/(\triangle T_{max}Fr^{2/5})$. Fig.5 exhibits the relationship between the dimensionless excess ceiling temeprature and distance away from reference position under typical mainline slope of 0% and 7%. The dimensionless temeprature rise along mainline tunnel can be well correlated utilizing the sum of two exponential funations taking the $Fr^{2/5}$ into account. That the dimenisonless temeprature rise along the mainline donstream has been normalized utilizing the sum of two exponential functions under all mainline slope, and the coeffcinets is shown in Table 2.



(a) Mainline slope of 0% (b) Mainline slope of 7%

Fig.5 Relationship between $\triangle T_x/(\triangle T_{max}Fr^{2/5})$ and $(x\text{-}x_0)/H_{ef}$ under typical conditions.

There are some difference of the coefficients in Eq. (1) between horizontal tunnel

and sloped tunnel. Thus, the pieswise function was developed for temeprature longitudinal decay inside mainline region. For horiozntal mainline, the temeprature longitusinal decay can be expressed as Eq. (8). For the inclined mainline, the exponential coefficients of b_1 and b_2 are similar under all tunnel slope conditions, thus, the average value are selected as the coefficients, given by b_1=-0.6 and b_2=-0.032. The constant coeffcients fo a_2 is 0.77 under all mainline slopes. The coeffciient of a_1 linearly decreases with the mainline slope, which can be normalizned by utilizing the sine of slopes, as shown in Fig. 6. Furthermore, the coefficient of a_1 equals to 2.61-2.35sinθ. Therefore, the temeprature longitudinal decay in sloped mainline can be expressed as Eq. (9).

For horizontal mainline tunnel,

$$\frac{\Delta T_x}{\Delta T_{\max} Fr^{2/5}} = 1.98\exp(-0.72\frac{x-x_{\max}}{H_{ef}}) + 0.77\exp(-0.05\frac{x-x_{\max}}{H_{ef}}) \quad (8)$$

For inclilned mainline tunnel,

$$\frac{\Delta T_x}{\Delta T_{\max} Fr^{2/5}} = (2.61-2.35\sin\boldsymbol{\theta})\exp(-0.6\frac{x-x_{\max}}{H_{ef}}) + 0.77\exp(-0.032\frac{x-x_{\max}}{H_{ef}}) \quad (9)$$

Table 2 Coefficients for $\Delta T_x/(\Delta T_{max} Fr^{2/5})$ under different mainline slope.

Coefficients	0%	1%	3%	5%	7%
a_1	1.98	2.59	2.54	2.49	2.45
a_2	0.77	0.77	0.77	0.77	0.77
b_1	-0.72	-0.59	-0.61	-0.6	-0.61
b_2	-0.05	-0.031	-0.034	-0.031	-0.033

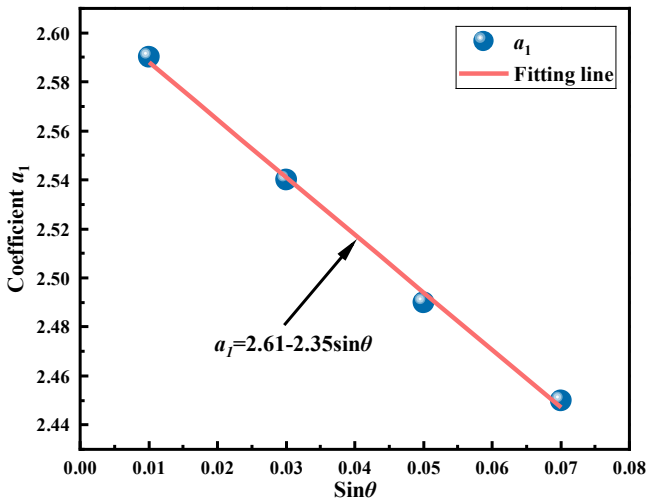
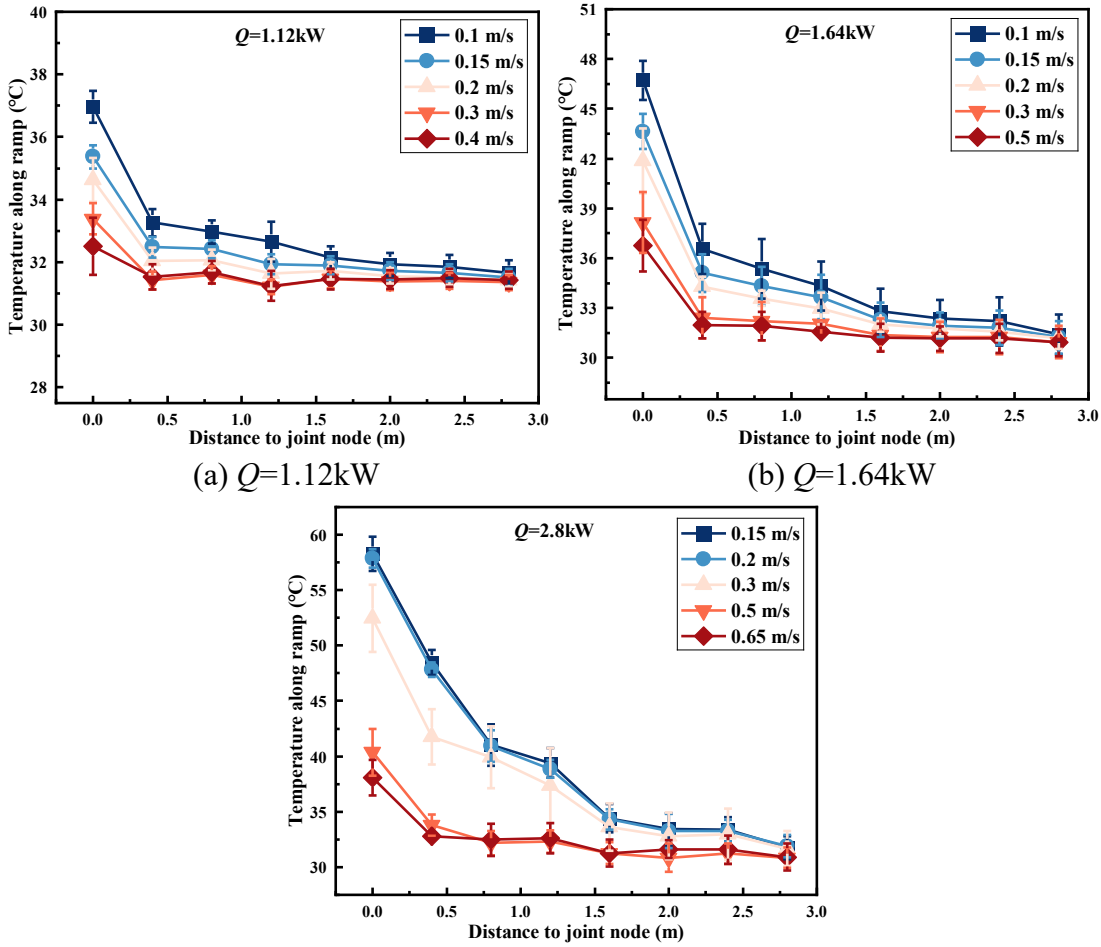


Fig.6 Relationshipe bettween coefficient a_1 and sinθ.

3.2 Temperature longitudinal decay in ramp

The temperature distribution in ramp for horizontal bifurcation tunnel has been studied in previous work [17, 39]. Thus, this study mainly focused on the effect of mainline slope on the temperature longitudinal distribution in ramp. Fig.7 exhibits the temperature longitudinal decay along ramp ceiling under different mainline slopes. The error bars are plotted to display the temperature difference as the mainline slope rises

from 1% to 7%. The temperature beneath the ramp ceiling is higher under greater fire power that indicates the more smoke enters the ramp region. The temperature in ramp is significantly decreased as the higher airflow velocity because of both the shearing effect near ramp entrance and cooling effect enhanced. For fire power of 2.8kW, the temperature in ramp decreased to ambient value away from joint node 0.8 m that indicates the airflow velocity arrive the critical value to control the smoke entering to ramp. The temperature beneath the ramp ceiling is slightly lower under steeper mainline conditions due to the larger induced airflow velocity. In total, the effect of mainline slope on the temperature distribution in ramp is weakly. However, Chen et al. [18] found the ramp slope has a significantly influence on the ramp temperature as the more smoke entering into ramp under steeper ramp slope.



(a) Q=1.12kW (b) Q=1.64kW

(c) Q=2.8kW

Fig.7 Temperature longitudinal distribution along ramp.

The temperature longitudinal decay in ramp has been corrected using an exponential correlation by Chen et al.[18], expressed as Eq. (10). Huang et al.[39] also normalized the temperature longitudinal decay in ramp using the $(x\text{-}x_0)/H_{ef}$. However, the previous study only considered the temperature distribution in ramp under natural condition. The present study takes the airflow velocity entering from mainline into account that the temperature at entrance node was selected as reference point. The temperature at reference position and in ramp also decreased as the cooling effect under higher airflow velocity, thus, the dimensionless temperature longitudinal decay is slightly impacted by

airflow velocity, as shown in Fig. 8. The dimensionless temperature longitudinal decay under each condition is corrected by utilizing $(x\text{-}x_0)/H_{ef}$. Fig.8 exhibits the dimensionless temperature longitudinal decay along ramp with mainline slope of 1%. The longitudinal decay rate of dimensionless temperature in ramp is different under various heat release rates. The decay coefficients under all mainline conditions are fitted and plotted in Fig.9. For a given heat release rate, the longitudinal temperature decay correction coefficients in ramp are closed as the mainline slope increases, suggesting the effect of mainline slope on temperature decay along ramp ceiling is weak. Thus, the average values of coefficients are selected to establish an exponential formula for temperature longitudinal decay and formulated by dimensionless heat release rate.

$$\frac{\Delta T_x}{\Delta T_0} = b\,\mathrm{e}^{-k(x-x_0)} + a \tag{10}$$

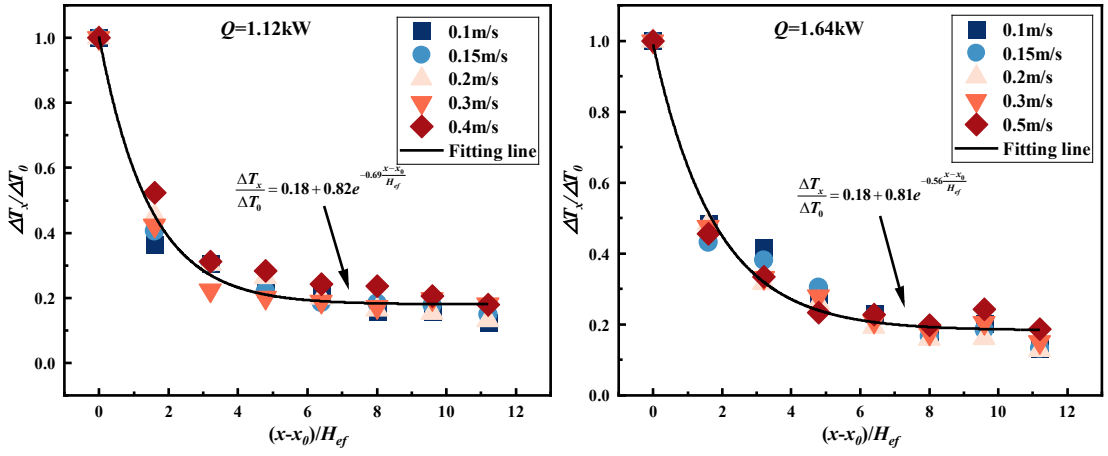
where $\triangle T_0$ is the temperature rise at reference point in K.

From Fig.9, the coefficients of a and b are very close to each other under different fire source powers. Thus, the average value of coefficients a and b can be taken as the fitting coefficient, which are 0.15 and 0.84. The exponential coefficient of k is lower under heat release rate of 2.8 kW than that value under 1.12 kW and 1.64 kW. Therefore, the dimensionless heat release rate Q^* was employed to correlate coefficient k. Fig.10 presents the relationship between k and Q^* that can be well expressed using the exponential formula, given as,

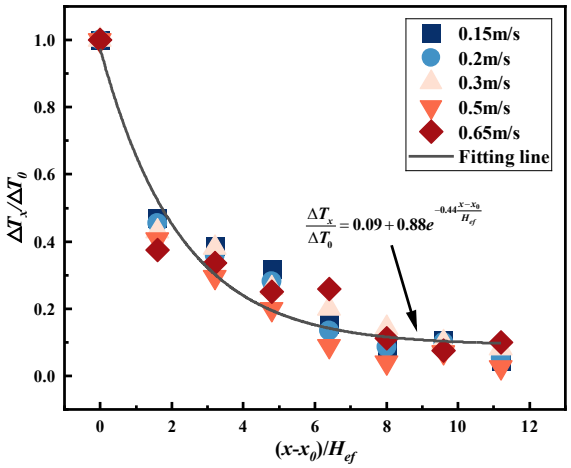
$$k = 0.81 - 0.001\mathrm{e}^{70.54Q^*} \tag{11}$$

Substitute a=0.15, b=0.84 and Eq.(11) into Eq.(10), as well utilizing $(x\text{-}x_0)/H_{ef}$ replacing $(x\text{-}x_0)$, the dimensionless temperature rise in ramp can be given as Eq. (12).

$$\frac{\Delta T_x}{\Delta T_0} = 0.15 + 0.84\,\mathrm{e}^{-\left(0.81-0.001e^{70.54Q^*}\right)\left(\frac{x-x_0}{H_{ef}}\right)} \tag{12}$$



(a) Q=1.12kW (b) Q=1.64kW



(c) Q=2.8kW

Fig.8 Relationship between $\triangle T_x/\triangle T_0$ and $(x\text{-}x_0)/H_{ef}$ with mainline slope of 1%.

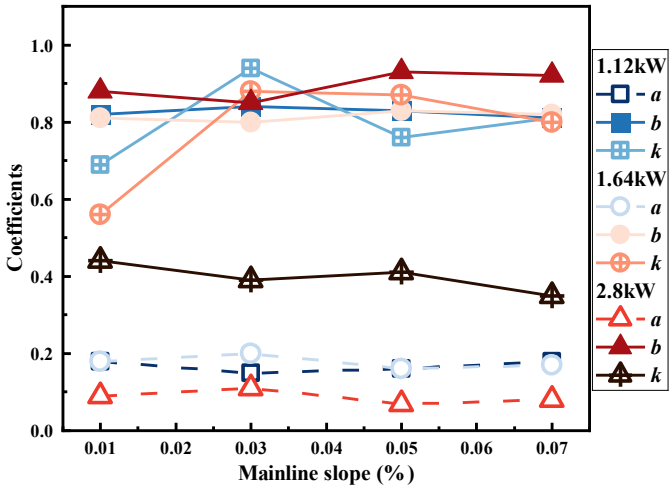


Fig.9 Temperature decay correction coefficients vs mainline slope.

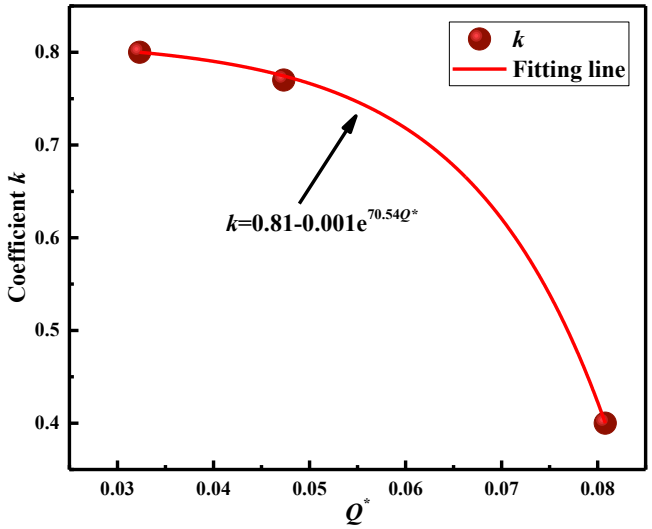


Fig.10 Relationship between coefficient k and Q^*.

4. Conclusions

This study conducted a series of small-scale fire experiments in a branched tunnel to investigate the temperature profile in a branched tunnel. The effect of mainline slope

and longitudinal ventilation velocity on temperature profile has been analyzed and developed the empirical model for maximum temperature. The main conclusions are summarized as follows:

(1) The maximum temperature beneath the tunnel ceiling increases with the heat release rate and decreases with lager longitudinal ventilation velocity. The effect of mainline slope on maximum temperature has been expressed by using the u_{in}, which related to $\sin^{0.36}\theta$.

(2) The temperature longitudinal decay along mainline is significantly influenced by the longitudinal ventilation and mainline slope. The $Fr^{-2/5}$ can normalize the temperature longitudinal decay along mainline downstream region where the sum of two exponential functions is established to predict the temperature longitudinal distribution.

(3) The temperature beneath the ramp ceiling decreases with increasing longitudinal ventilation velocity but increases with the fire power. The temperature inside ramp drops to ambient value as the airflow velocity achieving critical threshold for controlling smoke entry into the ramp. The exponential equation is established to predict the temperature longitudinal decay along ramp.

The present study clarified the temperature profile in a bifurcation tunnel fire with sloped mainline. This study contributes to fire risk assessment and guidance for fire protection system design. However, the fire location, ramp slope and lateral smoke exhaust affect the fire behaviors and temperature profile, which will be further investigated in the future.

CRediT authorship contribution statement

Zhiwen Wang: Writing – original draft, Methodology, Formal analysis, Conceptualization. **Youbo Huang**: Writing – original draft, Funding acquisition, Investigation, Data curation. **Yujia Zhao**: Writing – review & editing, Investigation. **Jingtai Shi**: Writing – review & editing. **Mengmeng Xie**: Writing – review & editing, Investigation, Data curation.

Declaration of Competing Interest

The authors declare that they have no known competing financial interests or personal relationships that could have appeared to influence the work reported in this paper.

Acknowledgements The

The authors acknowledge the supported by Natural Science Foundation of Chongqing, China [Grant No. CSTB2025NSCQ-GPX0214], the Science and Technology Research Program of Chongqing Municipal Education Commission (Grant No. KJQN202401523), Special Funding for Post-doctoral Research Projects in Chongqing (Grant No. 2024CQBSHTB3141).

Reference

[1] K. Wu, G. Wang, J. Li, L. Jiang, G. Wang, T. Zhang, Smoke bifurcation-induced low-temperature region in longitudinally ventilated tunnel fires: Phenomenon, modelling, and full-scale demonstration, 2026, 168: 107147.

[2] H. Wu, Z. Wang, J. Ji, C. Ye, K. Wang, Predicting fire dynamics in ventilated

tunnels with spatio-temporal buffer network, 2026, 168: 107079.
[3] Y. Huang, C. Luo, F. Tang, X. Liu, B. Dong, H. Zhong, Estimating the flame length and ceiling maximum temperature in a branched tunnel fire with sloped mainline before shunting, 2025, 322: 135655.
[4] L. H. Hu, R. Huo, Y. Z. Li, H. B. Wang, W. K. Chow, Full-scale burning tests on studying smoke temperature and velocity along a corridor, 2005, 20: 223–229.
[5] H. Li, Y. Xie, Z. Zhang, R. Li, H. Zhang, Investigating the Evolution of arch temperature and prediction model for temperature rise of fire Smoke: Model testing of an Extra-Long highway tunnel with vertical shaft, 2025, 113: 109781.
[6] L. Yu, X. Lei, L. Wang, P. Huang, C. Liu, Numerical investigation on the maximum and longitudinal distribution of ceiling gas temperature in an inclined tunnel: The combination effect of tunnel slope and longitudinal fire location, 2025, 163: 106685.
[7] R. L. Alpert, Calculation of response time of ceiling-mounted fire detectors, 1972, 8: 181–195.
[8] R. L. Alpert, Turbulent ceiling-jet induced by large-scale fires, 1975, 11: 197–213.
[9] H. Kurioka, Y. Oka, H. Satoh, O. Sugawa, Fire properties in near field of square fire source with longitudinal ventilation in tunnels, 2003, 38: 319–340.
[10] L. H. Hu, R. Huo, W. Peng, W. K. Chow, R. X. Yang, On the maximum smoke temperature under the ceiling in tunnel fires, 2006, 21: 650–655.
[11] Y. Z. Li, H. Ingason, The maximum ceiling gas temperature in a large tunnel fire, 2012, 48: 38–48.
[12] L. H. Hu, W. Tang, L. F. Chen, L. Yi, A non-dimensional global correlation of maximum gas temperature beneath ceiling with different blockage-fire distance in a longitudinal ventilated tunnel, 2013, 56: 77–82.
[13] W. Jiao, C. Chen, Z. Lin, Y. Bao, L. Shi, Experimental study on the burning characteristics and smoke temperature distribution of continuous spill fires in sloped tunnels, 2024, 152: 105884.
[14] Z. Gao, J. Jie, H. Wan, J. Zhu, J. Sun, Experimental investigation on transverse ceiling flame length and temperature distribution of sidewall confined tunnel fire, 2017, 91: 371–379.
[15] X. Fan, F. Tang, C. Shi, N. Zhu, Y. Huang, L. Hu, Impact of sub-atmospheric pressure on fire hazard and flow field characteristics in arced channel fires: ceiling temperature, flame extension and prediction models, 2025, 333: 137160.
[16] Y. Zhang, S. Xing, R. Chen, L. Chen, T. Li, P. Mao, Experimental study on maximum temperature beneath tunnel ceiling under the condition of double fire sources, 2020, 106: 103624.
[17] Z. Li, Y. Zhang, Y. Gao, L. Chen, T. Li, Study the maximum temperature of diffusion smoke downstream in a longitudinal ventilated branched tunnel with different transverse fire locations, 2024, 146: 105663.
[18] C. Chen, Y. Nie, Y. Zhang, P. Lei, C. Fan, Z. Wang, Experimental investigation on the influence of ramp slope on fire behaviors in a bifurcated tunnel, 2020, 104: 103522.
[19] H. Ingason, Y. Z. Li, Model scale tunnel fire tests with longitudinal ventilation,

2010, 45: 371–384.
[20] L. H. Hu, F. Tang, D. Yang, S. Liu, R. Huo, Longitudinal distributions of CO concentration and difference with temperature field in a tunnel fire smoke flow, 2010, 53: 2844–2855.
[21] L. H. Hu, R. Huo, W. K. Chow, Studies on buoyancy-driven back-layering flow in tunnel fires, 2008, 32: 1468–1483.
[22] X. Zhang, C. Shi, L. Hu, Temperature profile of impingement flow in the corner between wall and inclined ceiling induced by gaseous fuel jet flame, 2020, 259: 116232.
[23] L. H. Hu, R. Huo, H. B. Wang, Y. Z. Li, R. X. Yang, Experimental studies on fire-induced buoyant smoke temperature distribution along tunnel ceiling, 2007, 42: 3905–3915.
[24] M. A. Delichatsios, The flow of fire gases under a beamed ceiling, 1981, 43: 1–10.
[25] J. Ji, H. Wan, K. Li, J. Han, J. Sun, A numerical study on upstream maximum temperature in inclined urban road tunnel fires, 2015, 88: 516–526.
[26] C. Chen, W. Jiao, Y. Zhang, P. Lei, A comparative study on smoke temperature profile and corresponding different-exponential form correlation in single-line and bifurcated tunnel fires, 2023, 136: 105090.
[27] Z. Li, Y. Gao, X. Li, P. Mao, Y. Zhang, K. Jin, T. Li, L. Chen, Effects of transverse fire locations on flame length and temperature distribution in a bifurcated tunnel fire, 2021, 112: 103893.
[28] Y. Huang, Y. Li, J. Li, K. Wu, H. Li, K. Zhu, Experimental study on the temperature longitudinal distribution induced by a branched tunnel fire, 2021, 170: 107175.
[29] Z. Gao, H. Wan, J. Ji, The effect of blend ratio on the combustion process of mutually stratified blended fuels pool fire, 2021, 38: 4995–5003.
[30] K. Wu, L. Liu, M. Yin, K. Zhu, X. Zhang, G. Wang, Prediction of maximum ceiling temperature rise in inclined tunnel fire based on improved non-orthogonal ventilation plume model, 2026, 172: 107500.
[31] Y. Huang, Y. Li, J. Li, K. Wu, K. Zhu, H. Li, Modelling and experimental investigation of critical velocity and driving force for preventing smoke backlayering in a branched tunnel fire, 2020, 99: 103388.
[32] J. Kong, Z. Xu, W. You, B. Wang, Y. Liang, T. Chen, Study of smoke back-layering length with different longitudinal fire locations in inclined tunnels under natural ventilation, 2021, 107: 103663.
[33] B. Merci, One-dimensional analysis of the global chimney effect in the case of fire in an inclined tunnel, 2008, 43: 376–389.
[34] L. H. Hu, L. F. Chen, L. Wu, Y. F. Li, J. Y. Zhang, N. Meng, An experimental investigation and correlation on buoyant gas temperature below ceiling in a slopping tunnel fire, 2013, 51: 246–254.
[35] C. Chen, T. Lu, Y. Zhang, C. Shi, W. Jiao, Experimental study on temperature profile and critical velocity in bifurcated tunnel fire with inclined transverse cross-passage, 2023, 186: 108120.
[36] M. Qiu, Y. Li, Z. Su, H. Zhong, H. Zhao, H. Zhu, Influence of tunnel slope on smoke propagation characteristics and longitudinal ceiling temperature profile in

metro carriage fires, 2026, 169: 107269.
[37] P. Li, L. Shang, D. Yang, W. Zhang, Experimental study and modelling on critical velocity, smoke temperature distribution and driving force in uphill tunnel fire with longitudinal ventilation, 2026, 160: 104602.
[38] S. Zhao, F. Liu, F. Wang, M. Weng, Experimental studies on fire-induced temperature distribution below ceiling in a longitudinal ventilated metro tunnel, 2018, 72: 281–293.
[39] Y. Huang, P. Lai, C. Xiang, B. Dong, H. Zhong, F. Tang, Thermal runaway behaviour of lithium-ion batteries in branched tunnels: Influence of cathode chemistry and charge/discharge rate, 2026, 354: 141057.